JOURNAL OF MATERIALS SCIENCE 35 (2000) 1389–1396

Silica coatings on bismaleimide (BMI) polymeric substrates

C. MUKHERJEE, E. D. CASE*, A. LEE
Materials Science and Mechanics Department, Michigan State University, East Lansing, MI, 48824, USA
E-mail: casee@egr.msu.edu

For many years, ceramics have been added to polymeric materials as reinforcements or extenders. Recently, thin ceramic coatings have been applied to polymers for biomedical applications, and in this paper ceramic coatings are applied to an aerospace polymer, bismaleimide (BMI). Unreinforced BMI specimens were coated with a thin, protective layer of a dense silicate ceramic material. Vickers indentation testing on the coated and uncoated BMI specimens indicated that the coatings adhere surprisingly well to the substrate, with cracking of the coating taking place only within a diamond-shaped region with diagonal dimensions equivalent to the Vickers indentation impression.

1. Introduction

1.1. Ceramic/polymer material systems and applications

Ceramics and polymeric materials have been used in combination for decades, such as in the case of fiberglass, where ceramic (glass) fibers reinforce polymer matrices. Also, powdered silica, calcium carbonate, and clay are widely used as inexpensive extenders for polymers [1] while mica platelet additions can increase a polymer's impact strength, flexural modulus, and improve resistance to chemical attack [2]. For biomedical use, several weight percent barium sulfate ($BaSO_4$) dispersed in polymethyl methyacrylate (PMMA) bone cement makes the cement radiopaque and thus renders the bone cement "readable" on medical x-rays [3]. Each of these applications involve adding ceramics in particulate, fiber, or platelet form to the bulk of a polymeric material. However, applying adherent ceramic coatings to polymers is a relatively recent development.

Duchatelard *et al.* applied thin alumina films to PMMA using RF magnetron sputtering [4, 5] for medical applications. As is the case with ceramic coatings on metals [6], ceramic coatings on polymers enhance biocompatibility [4, 5]. In addition, alumina coatings improve the wetability of PMMA, which is an advantage for dental uses, where saliva wetability of materials is quite important [5]. Rather than medical applications, this paper focuses on the fabrication and indentation testing of thin, adherent ceramic coatings on bismaleimide (BMI). BMI is a polymer used for aerospace applications due to its (i) ease of processing and (ii) excellent high temperature properties. Prior to crosslinking, BMI is a viscous liquid, enabling BMI to be processed with methods similar to those used to process epoxy resin. Upon curing, the glass transition temperature of BMI is about 300°C, which is quite high for a polymer.

Although BMI is easily processed and has good high temperature properties, the physical and mechanical properties of BMI are affected by organic solvents and moisture [7], as is the case for many polymeric systems. Also, BMI and BMI-carbon composites are susceptible to galvanic corrosion. The goal of this research is to produce a thin continuous, electrically insulating surface coating on BMI that is sufficiently adherent and robust with respect to various erosion and abrasion damage sources that it might reduce moisture/solvent ingress as well as galvanic corrosion. The focus in this paper is on producing a crack-free ceramic coating on BMI substrates and evaluating the coating robustness via Vickers indentation.

1.2. Bismaleimide chemistry

The cure reaction characteristics and kinetics in the liquid and glassy-state of bismaleimidodiphenylmethane (BMPM)-diallyl bisphenol alcohol (DABPA) BMI composite matrices have been studied by Fourier transform infrared spectroscopy (FTIR), differential scanning calorimetry (DSC) and gel permeation chromatography (GPC) [8–12]. In the 100 to 200°C range the BMPM reacts with the DABPA to form an "ene" adduct. The "ene" adduct is pentafunctional as a result of (i) three carbon-carbon double bonds, capable of chain extension and crosslinking, and (ii) two hydroxyl groups capable of etherification by hydroxyl dehydration.

BMI is a crosslinked polymer glass and as such its mechanical properties depend on the detailed topography of the crosslinked network [13]. For example, depending on the curing conditions, the elastic modulus

* Author to whom all correspondence should be addressed.

of BMI varies from 3.55 GPa to 4.12 GPa [7] and the room temperature density ranges from 1.2375 g/cm^3 to 1.2473 g/cm^3 [14].

The relative reaction rates for the liquid-state and the principal cure reactions involving the five reactive "ene" group species have been fully characterized in the 200 to 350°C temperature range [12]. Morgan *et al.* [8] used the infrared bands at 3473 cm^{-1} and 1179 cm^{-1} to monitor the disappearance of hydroxyl groups and appearance of the ether groups respectively for the etherification reaction by hydroxyl dehydration. Recent work [12] has identified infrared bands associated with the cure reactions of the allyl (A) at 915 cm^{-1} and 995 cm^{-1}, propenyl (B) at 931 cm^{-1} and 975 cm^{-1} and maleimide (C) at 690, 713, 827 and 1639 cm^{-1} double bonds respectively.

2. Experimental procedure

2.1. Materials

The Bismaleimide (BMI) resin system used in this study (MatrimidTM 5292, Ciba-Geigy [15]) was a two component system based on 4,4′-bismaleimidodiphenylmethane (BMPM) and 0,0′-diallyl bisphenol alcohol (DABPA). The DABPA amber viscous liquid monomer was poured into a magnetic stir-activated beaker and heated on a hot plate at 130°C, then yellow BMPA crystalline powder was added slowly and mixed until a homogeneous solution was achieved. This prepolymer mixture was degassed in a vacuum oven set at a temperature of 30°C for 20 minutes. This mixture was then poured into a preheated (90°C) mold and cured in a nitrogen atmosphere oven for 1 hour at 177°C followed by an additional 1 hour cure at 200°C. During processing, the stoichiometric ratio of BMPA : DABPA was varied such that the BMI specimens included in this study had BMPM : DABPA ratios of 1 : 0.82, 1 : 1 and 1 : 1.13. The three stoichiometric ratios were included in this study in order to determine if the BMPM: DABPA ratios affected either (1) the coating morphology or (2) the adhesion of the film, where the film adhesion for each of the substrate chemistries was tested by point contact loading (Vickers indentation).

The silica coatings that were applied to the BMI were an organic-based liquid that was spun onto the BMI substrates. The liquid is converted to an amorphous silica film upon pyrolysis.

2.2. Specimen preparation

Using a low speed diamond saw, the uncoated BMI substrates were cut into sections approximately 1 cm × 1 cm × 0.4 cm. During cutting, water was used as coolant instead of oil to prevent contamination of the BMI. After sectioning with the diamond saw, one of the substrate's 1 cm × 1 cm faces was first ground using a 600-grit abrasive paper and then polished using 5 μm, 0.3 μm, and 0.05 μm alumina abrasive powders.

The polished BMI specimens were precured prior to coating in order to reduce shrinkage of the BMI during the subsequent coating procedure. The precuring was done in air for 60 to 120 minutes in a resistively heated oven at temperatures ranging from 180°C to 265°C.

The polished BMI surfaces first were cleaned with deionized water, then cleaned with acetone, and then blotted dry with a paper towel. While several of the BMI substrates were left uncoated for subsequent testing, most of the substrates were coated with the silica film solution immediately after cleaning. Five to six drops of silica film solution were applied to the center of the BMI substrate using a pipette. The specimens were then spun on a commercial substrate spinner at rates ranging from approximately 500 rpm to 4000 rpm. The specimen coatings then were cured in air in a resistively-heated oven at 150°C for 20 minutes, producing a brittle silicate film.

2.3. Vickers indentation damage

Both uncoated and coated BMI specimens were indented following polishing, cleaning, and precuring. A commercial hardness tester (Buehler Semimacro indentator, Lake Bluff, IL) was used to indent both the uncoated and coated specimens using a loading rate of 70 microns per second, a loading time of 10 seconds and loads from 2.94 N to 98 N. The dimensions of the resulting crack damage were measured using a digital readout attachment to the Vickers indentor, which can be read to ±0.1 micron.

2.4. Coating thickness measurements

A Scanning Electron Microscope (SEM) and an Environmental Scanning Electron Microscope (ESEM) were used to determine the silica coating thickness. BMI specimens precured at 200°C for 1 hour were coated at spinning speeds varying from 500 rpm to 4000 rpm and then cured in air at 150°C for 20 minutes. The coated specimens were sectioned, using a low speed diamond saw, so that the thickness values could be measured near the center of the specimen.

Coated BMI specimens were then placed in the ESEM at tilt angles varying from 7° to 12° in order to facilitate the coating thickness measurements. The true thickness h is given by $h = h_W/\cos\theta$ where h_W is the measured coating thickness and θ the tilt angle in the ESEM.

Since the ESEM allows observation of nonconductive specimens without an electrically-conductive coating, no conductive coating was applied to the surfaces of either the silica coated or the uncoated BMI specimens. The lack of a conductive coating is an advantage in this study, as such a coating could obscure details of cracks and other surface features on the BMI specimens.

3. Results

3.1. Coating thickness effects

Spin rates between 500 rpm and 4000 rpm produced (after curing) coating thickness from 2.5 microns to 0.15 microns (Fig. 1). The coating thickness was measured for a total of 18 BMI specimens with a BMPA : DABPA ratio of 1 : 1.13, where the average

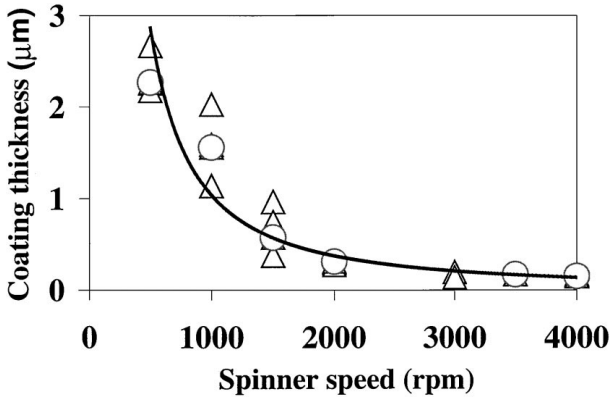

Figure 1 The thickness of silica coating on BMI substrate as a function of the spinning rate. The BMI (BMPM : DABPA = 1 : 1.13) substrates were first precured at 200°C for 1 hour, then the coated specimens were cured at 150°C for 20 minutes.

thickness value for each specimen (Fig. 1) was determined from the mean of at least six individual measurements. Similar values of coating thickness versus spin rate were found for the BMPA : DABPA ratio of 1 : 1.

For each of the three BMPA : DABPA ratios (1 : 0.82, 1 : 1 and 1 : 1.13) the nature of the coating as a function of spin rate was very similar. In particular, coatings ranging in thickness from 1.7 microns to 2.5 microns were discontinuous, as determined both by unaided eye observations and a 200 × optical microscope. Islands of silica coating (Fig. 2) were observed for coatings spun at 500 rpm and 1000 rpm. For the specimens spun at 500 rpm, the distance between the silica islands averaged about 12 microns, and for 1000 rpm specimen the distance between the islands was about 6.3 microns. Coatings spun at 1500 rpm (with a thickness 0.6 ≈ microns) displayed systems of parallel coating cracks with spacings between cracks of about 100 to 150 microns and with coating crack lengths ranging from 3 to 4 mm. These cracks also had occasional side branching cracks that ranged in length from about 1 mm to 2.5 mm. Coatings which had been spun between 2000 rpm and 4000 rpm had thicknesses ranging from 0.3 microns to 0.15 microns, and were smooth, continuous and crack-free as determined by examination via both optical microscopy and the ESEM.

3.2. Vickers indentation damage

While a number of studies have considered the indentation and nanoindentation behavior of brittle films on brittle substrates [16–18] and the behavior of free standing brittle films [19, 20], this study considers the indentation behavior of a brittle (silica) film on a relatively compliant substrate (the polymeric material, BMI). Vickers indentation loading yields at least a first approximation to point-contact loading damage induced by a variety of processes [21], including by handling components during fabrication and assembly of components, as well as damage accumulated in service and during maintenance. Thus, rather than test the mechanical properties of the coating itself (in which case a nanoindentation study would have been more important), it was the aim of this study to examine damage that breached the coating and to determine if such loading also caused damage (such as coating delamination) that extended far from the region of indentor contact.

In this study, both uncoated and silica-coated specimens of each of the three BMPM : DABPA stoichiometries (1 : 0.82, 1 : 1, and 1 : 1.13) were indented with an average of 6 to 10 indentations per load, at loads of 2.94 N to 98 N (Figs 3–8). For the coated specimens, a total of 296 indentations were made.

The uncoated specimens showed the indentation impression due to the square-pyramidal Vickers indent impression (Fig. 3). For a 49 N load, indentation diagonal

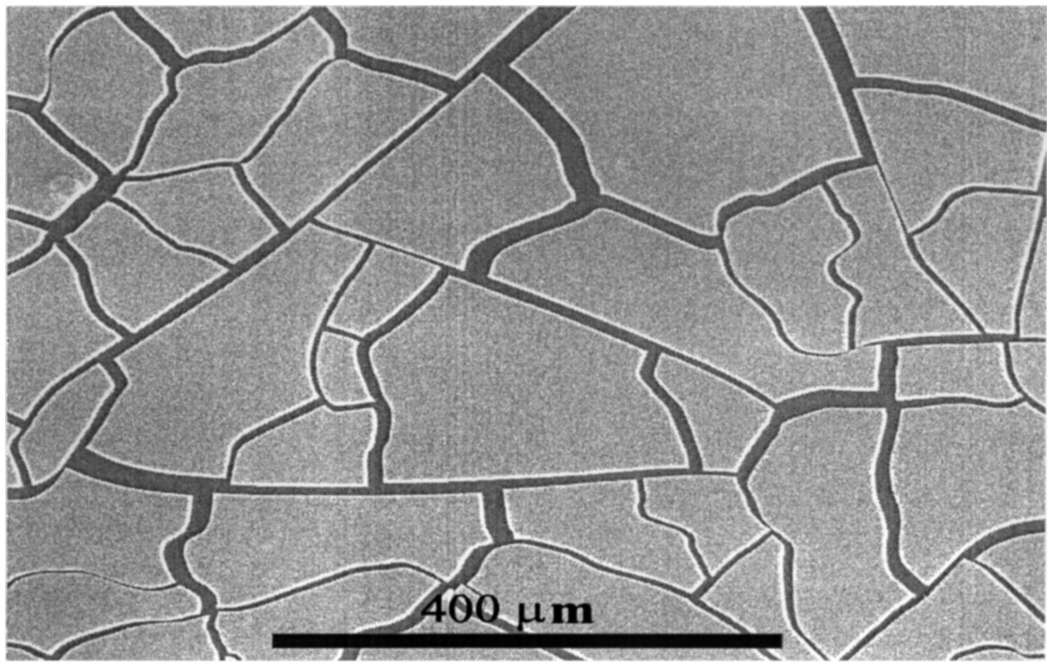

Figure 2 Micrograph of ≈2.5 micron thick silica coating on BMI showing separated islands of the coating. The specimen, with substrate stoichiometry BMPM : DABPA = 1 : 1, was precured at 200°C for 1 hour, coated at 500 rpm for 20 seconds and then cured at 150°C for 20 minutes.

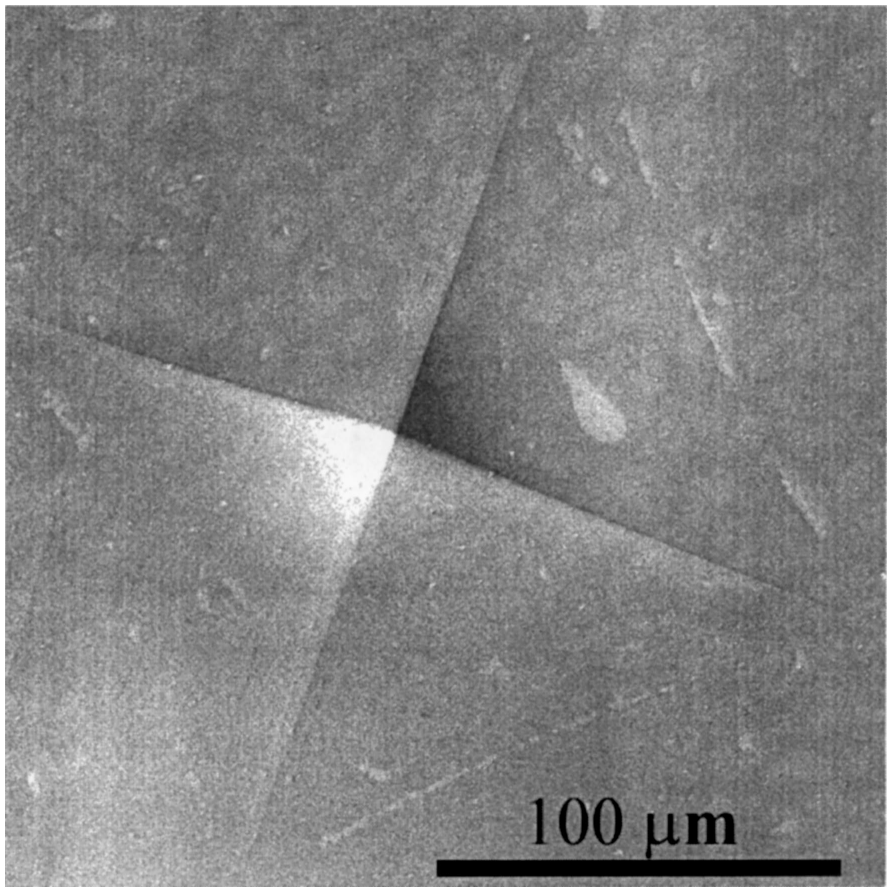

Figure 3 Micrograph of a Vickers indent made at a load of 49 N on an uncoated BMI specimen (BMPM : DABPA = 1 : 1). The BMI was precured at 200°C for 1 hour and again cured at 150°C for 20 minutes.

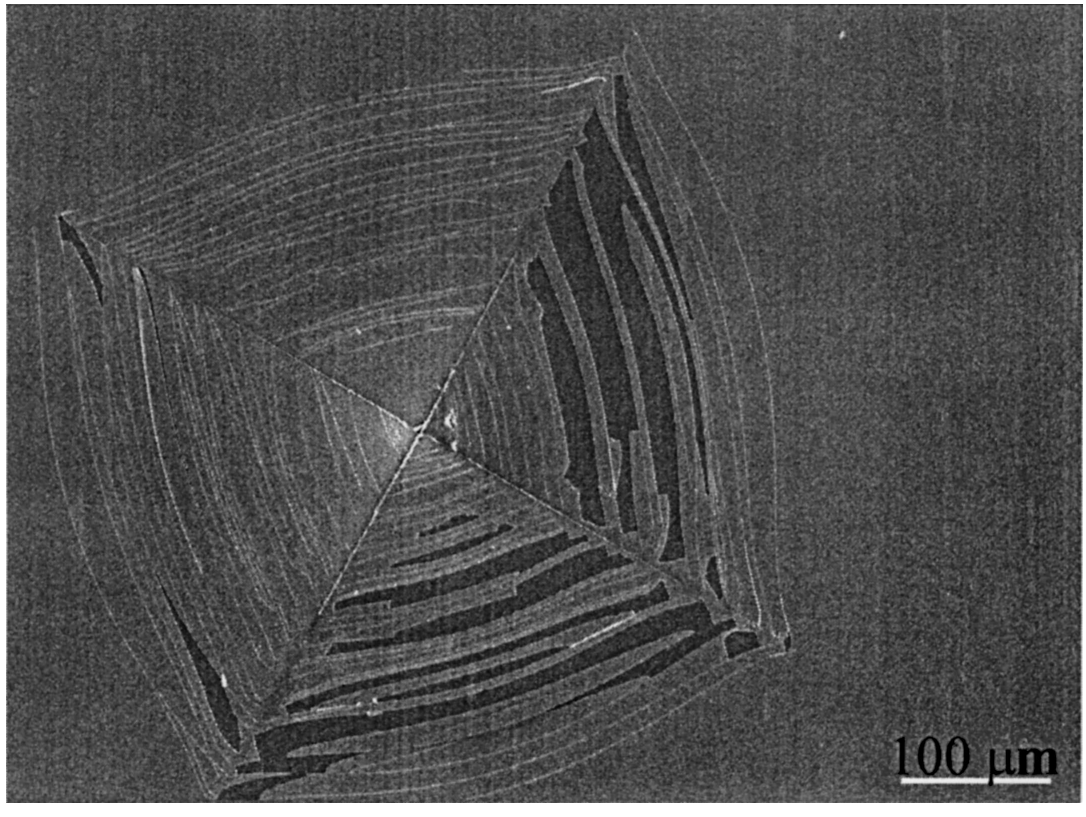

Figure 4 Micrograph of a Vickers indent made at a load of 49 N on a coated BMI specimen (BMPM : DABPA = 1 : 1), where the coating thickness was ≈0.17 microns. The specimen was precured at 200°C for 1 hour, coated at 3500 rpm for 20 seconds, cured at 150°C for 20 minutes.

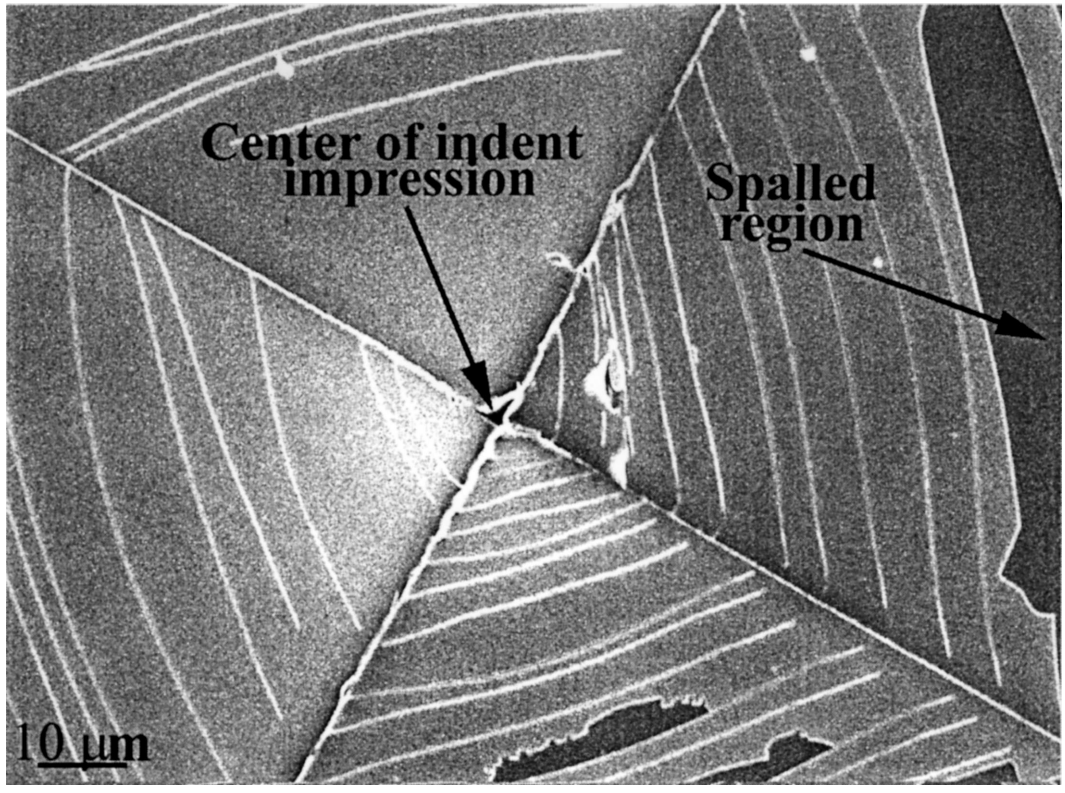

Figure 5 For the same indented specimen as shown in Fig. 6, a higher magnification view of the array of concentric cracks that comprise the indentation crack field. The center of the indent impression and a spalled region of the coating are shown.

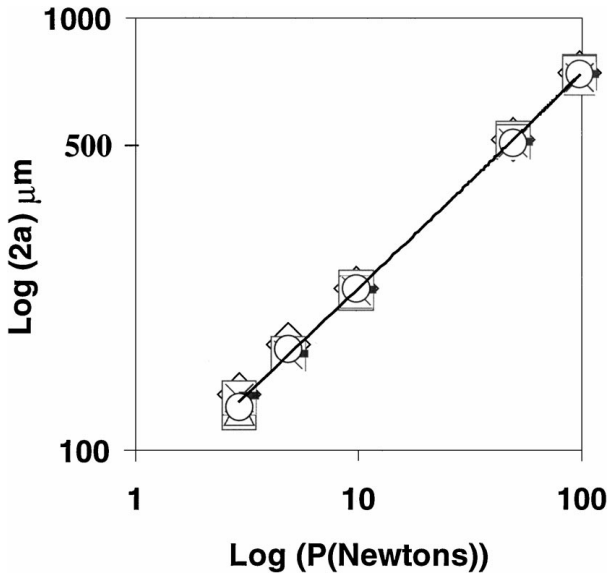

Figure 6 Logarithmic plot of indent dimension versus indentation load for (i) BMI (BMPM : DABPA = 1 : 0.82) uncoated but heated at 200°C for 1 hour and then reheated at 150°C for 20 minutes and for (ii) BMI (BMPM : DABPA = 1 : 0.82) precured at 200°C for 1 hour, coated at 3000 rpm for 20 seconds and then cured at 150°C for 20 minutes. Loads were varied from 2.94 N to 98 N. The solid curve represents a least-squares fit of the data to Equation 1.

length, $2a$ (Fig. 3), for the uncoated BMI was about 520 microns. For the silica-coated specimens, Vickers indentation produced cracks in the silica coating in a pattern of concentric diamond-shaped cracks, centered on the indent impression (Figs 4 and 5). The outermost cracks in the diamond-shaped array tend to bow outward slightly (Figs 4 and 8) while the bowing seems less pronounced toward the center of the indent impression (Fig. 5).

For a given Vickers indentation load, the diagonal length of the array of diamond shaped cracks corresponded very well with the diagonal length of the uncoated BMI specimens (Fig. 6). In order to compare the indentation diagonal for the uncoated specimens with the diagonal length of the coating-crack region, let

$$2a_{\text{uncoat}} = \text{indentation diagonal (uncoated specimens)}$$

and

$$2a_{\text{coat}} = \text{diagonal length of the diamond-shaped coating-crack region.}$$

In this study, for a given indentation load

$$a_{\text{uncoat}} \cong a_{\text{coat}}.$$

For the entire set of indentations included in this study, $\langle |a_{\text{uncoat}} - a_{\text{coat}}| \rangle$, the mean of the absolute values of the differences between a_{uncoat} and a_{coat} was about 2.3 percent, while the mean difference $\langle a_{\text{uncoat}} - a_{\text{coat}} \rangle$ was about 0.2 percent. The maximum difference observed between a_{uncoat} and a_{coat} was about 9 percent, in the case of a single indentation at a load of 2.94 N, and in general the difference $a_{\text{uncoat}} - a_{\text{coat}}$ tended to be greater at 2.94 N that at the higher loads.

Except for one instance, no coating delamination was observed for the entire set of 296 indentations performed on the silica coating/BMI substrate system during this study. The lone example of coating

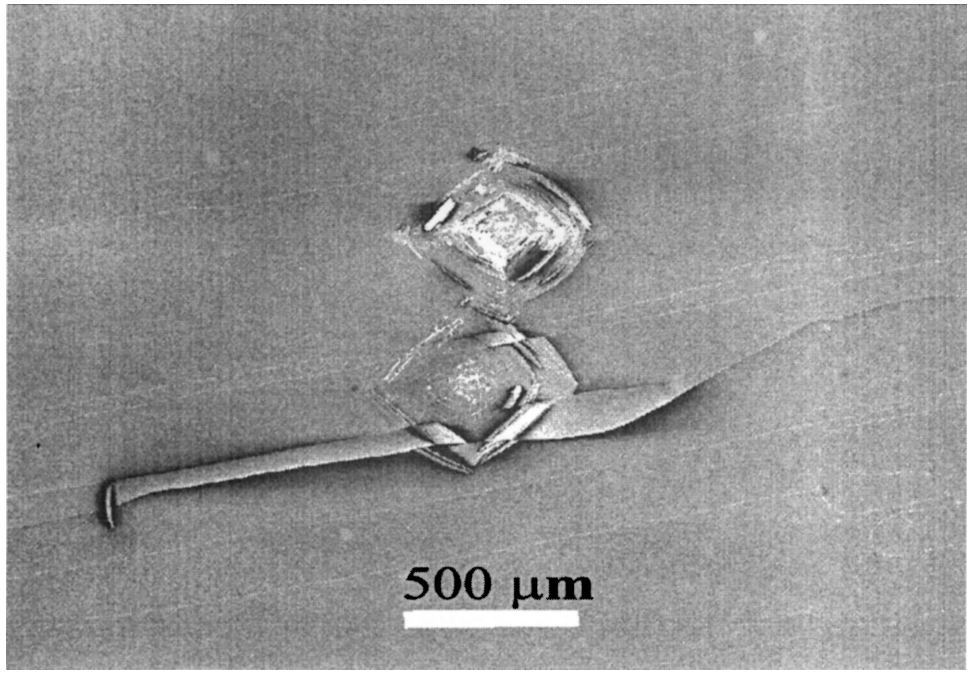

Figure 7 Micrograph showing a coating delamination and crack associated with a pair of closely spaced 49 N Vickers indentations on a BMI specimen (BMPM : DABPA = 1 : 1) which was precured, coated and cured using the same procedure as for the coated specimens in Fig. 5. This is the only example of a coating delamination that was observed in this study.

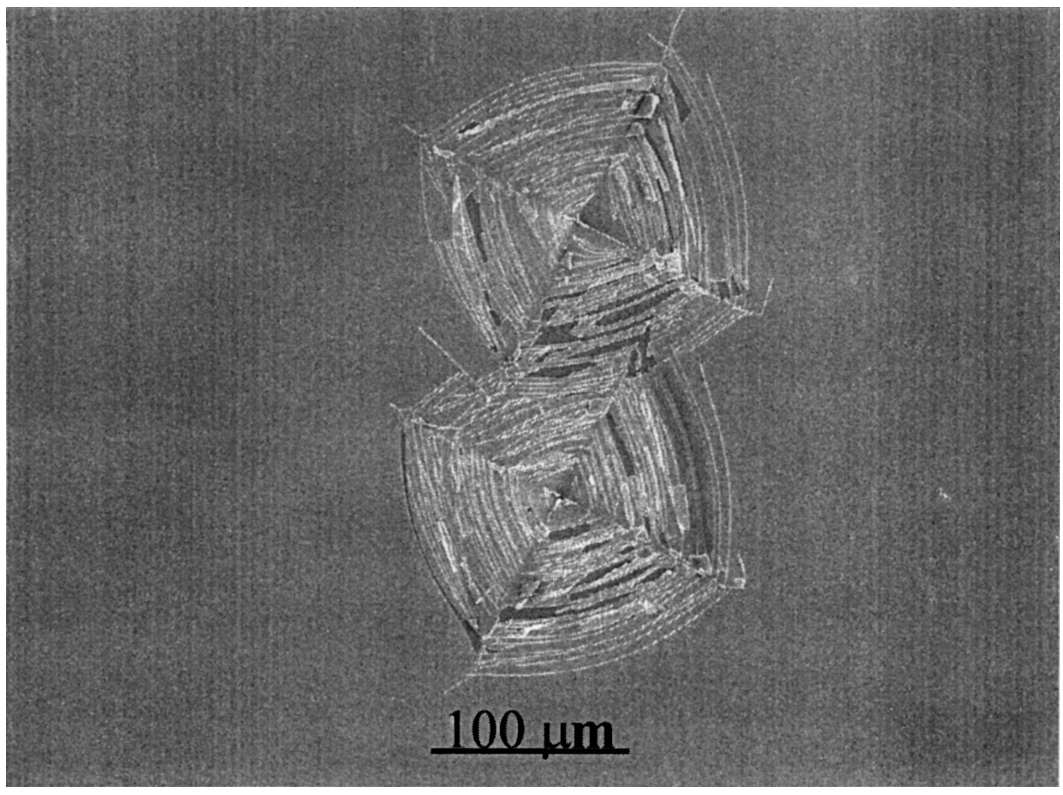

Figure 8 Micrograph showing closely-spaced indentations.

delamination occurred for a pair of 49 N Vickers indentations that were placed such that the edges of the coating-crack fields were essentially touching (Fig. 7). After observing the coating delamination for the pair of indentations shown in Fig. 7, we intentionally placed pairs (Fig. 8) and sets of four indentations with spacing similar to those shown in Fig. 7 in an effort to induce further coating delamination cracks, but none were apparent for closely-spaced indentations other than the particular pair of indentations shown in Fig. 7. Thus, the lack of coating delamination cracks for other closely-spaced indentation crack fields may indicate the delamination cracking shown in Fig. 7 may have resulted from an interfacial coating defect near the indentation site rather than indicating a general trend toward delamination.

A recent study by Li *et al.* [22] showed that, in agreement with the results of this study, hard coatings

on soft substrates tend to produce coating cracking rather than coating delamination. In the experimental portion of their work, Li *et al.* used a sharp indentor (Berkovich, three-sided pyramid) to indent 0.1 micron thick diamond-like-carbon (DLC) coatings on a polycarbonate substrate, at loads of up to 700 mN (0.7 N). Li determined the Young's moduli of the polycarbonate substrate and the DLC coating to be 3.3 GPa and 130 GPa, respectively [22]. The silica/BMI coating and substrate system indented in this study is similar to that studied by Li [22] in several respects, in that for this study the coating thickness ranged from about 0.3 to 0.15 microns, with indentations performed by a sharp (Vickers, four-sided pyramid) indentor for loads down to 2.94 N. Although the moduli of the coating and substrate were not determined in this study, the literature values for the elastic modulus of BMI (about 3.6 GPa to 4.1 GPa [7]) is similar to the 3.3 GPa obtained by Li *et al.* for the polycarbonate substrates [22]. The literature value of 72 GPa for the elastic modulus of fused silica [23] within a factor of two of the 130 GPa modulus that Li *et al.* measured for their DLC coating.

Although coating delamination was rarely observed in this study, within the boundaries of the diamond-shaped crack field on the indented coated, a limited spallation of the coatings was observed (Figs 4, 5 and 8). To quantify the extent of coating spallation, a BMI specimen with a coating thickness of 0.17 microns, indented at a 49 N load, was examined in the ESEM. Four micrographs were required to represent the entire diamond-shaped crack damage zone. Using a grid drawn on the four micrographs, the fractional spallation area, f_S, was estimated as 0.22. Although f_S was quantitatively determined for only one specimen, optical and SEM examinations of the indentation damage for the other coated specimens included in this study indicated qualitatively similar values of f_S. Thus, the area was very minor for the relatively severe loading state of the Vickers indention loads up to 98 N.

As determined by least-squares fitting, the load, P, versus indentation damage dimension (Fig. 6) was consistent with the relationship

$$P = 2Ba^n \tag{1}$$

where B is a constant and we let $a_{\text{uncoat}} = a_{\text{coat}} = a$, due to the agreement (noted above) between a_{uncoat}, the diagonal length of the indentation impression for the uncoated BMI specimens and a_{coat}, is the diagonal length of the concentric, diamond-shaped crack field for the silica-coated BMI specimens (Fig. 6). A least-squares fit of the data to Equation 1 yielded a value of 1.98 ± 0.02 for the exponent n and 317.5 MPa $\pm$ 50.0 MPa for the constant B. The least-squares fit values for n and B are suggestive of the functional form of load-indentation diagonal length relationships found in the literature for brittle materials [21], namely that

$$H = \frac{P}{2a^2} \quad \text{or} \quad P = 2Ha^2 \tag{2}$$

where the constant B would correspond to the hardness H, thus giving a hardness value of $H = 317.5$ MPa $\pm$ 50.0 MPa. Since the value of H is essentially the same for both the uncoated BMI specimens and the silica-coated BMI specimens (Fig. 6), one would assume that the value of 317.5 MPa $\pm$ 50.0 MPa corresponds the hardness of the BMI substrate itself. Also, since the thickness of the silica coatings on the indented specimens ranged from 0.15 to 0.3 microns, one would not expect the silica coating to significantly affect the value of H measured for Vickers indentation loads between 2.94 N and 98 N.

Although no hardness values for BMI are available in the literature, a hardness of about 318 MPa is consistent with the hardness values for other rigid polymers that are available in the literature. For example, recent Vickers indentation studies of an epoxy resin, an acrylic resin, and a series of aromatic polyesters give hardness values for those polymers of about 100 MPa to 300 MPa [24, 25]. In addition, given an elastic modulus, E, of BMI between about 3.6 and 4.1 GPa, the resulting H/E ratio is also consistent with the literature for the H/E ratios of rigid polymers [25].

Given the form of Equation 2, the approximately constant slope of the $\log(2a)$ versus $\log(P)$ plot in Fig. 6 implies that the hardness, H, of BMI is essentially independent of load, P, for the range of indentation loads employed in this study. This is consistent with data from the literature for other rigid polymers, where the hardness of PMMA, high density polyethylene, an epoxy resin and an acrylic resin is load-independent for higher Vickers indentation loads [24–27]. In particular, for a range of Vickers indentation loads very comparable to those employed in this study, (approximately 1 to 100 N, see Fig. 2 of reference [24]), Low *et al.* found that the measured hardness was independent of load for both an epoxy resin and an acrylic resin [24]. Low *et al.* did observe that the hardness of their epoxy resin and acrylic resin specimens was a function of loading time for the Vickers indentation loading, with the measured hardness decreasing by roughly 5-percent over the loading-time interval from 5 to 30 seconds [24]. However, all the indentations done in this study were performed with a load time of 10 seconds, so the loading time effects on the data in this study should be minimal.

4. Summary and conclusions

Using a spin-on process, unreinforced BMI polymeric substrates were coated with a silicate coating. For the specimens coated with a silica solution, curing at 150°C for 20 minutes produced silicate coatings roughly 0.15 to 2.5 microns thick. A concentric, diamond shaped array of cracks was induced in the silica coatings upon loading with a Vickers indentor (Figs 4, 5 and 8). Over a load range from 2.94 N to 98 N the diagonal length of the crack array, $2a_{\text{coat}}$, for the coated specimens were essentially identical to the diagonal length or the indentation impression of the uncoated BMI specimens, $2a_{\text{uncoat}}$ (Fig. 6). Within the coating-crack array there was only very minor spalling of the coating from the BMI substrate (roughly 22 percent) and coating delamination was observed for only one out of 296 indentation crack fields induced for Vickers indentation

over the entire load range of 2.94 N to 98 N. Thus, it appears that the silica coatings adhered exceptionally well to the polymeric substrates under point contact loading conditions.

The diagonal dimensions of the diamond-shaped coating-crack array, $2a_{coat}$, increased monotonically with load as described by Equation 1 (Fig. 6), where a least squares fit of the data gave $n = 2$. Thus, Equation 1 can be rewritten in terms of Equation 2, where the constant B (in Equation 1) may be interpreted as the hardness, H, of the BMI, where $H = 317.5\ \text{MPa} \pm 50.0\ \text{MPa}$. This hardness value for BMI is consistent with literature values for other rigid polymers [24–27].

Future work should include studies of coatings on reinforced BMI substrates. In addition, other coating chemistries (i.e. other than silicate coatings) should be investigated. The integrity of the coatings with respect to thermal shock and chemical attack would be of interest, in addition to studies of the point-contact loading damage.

Acknowledgements

The authors acknowledge the financial support of the Research Excellence Fund of the State of Michigan, administered through the Composite Materials and Structures Center. The authors also acknowledge Dr. Richard Schalek for his assistance with the Environmental Scanning Electron Microscope at the Composite Materials and Structures Center and Dr. Ki-Yong Lee for his assistance with some of the initial coating work on the BMI specimens.

References

1. J. CRAWFORD, "Plastics Engineering," 2nd ed., (Pergamon Press, Oxford, 1987) Ch. One.
2. M. MOSKOWITZ, *Plastics World* **51** (1993) 47.
3. J. B. PARK and R. S. LAKE, "Biomaterials," 2nd ed., (Plenum Press, New York, 1992) p. 154.
4. DUCHATELARD, G. BAUD, J. P. BESSE and M. JACQUET, *Thin Solid Films* **250** (1994) 142.
5. DUCHATELARD, G. BAUD, J. P. BESSE and M. JACQUET, *Journal of Dental Research* **74** (1995) 940.
6. P. WARD, K. N. STRAFFORD, T. P. WILKS and C. SUBRAMANIAN, *Journal of Materials Processing Technology* **56** (1996) 364.
7. E. E. SHIN, R. J. MORGAN, J. ZHOU, J. E. LINCOLN, R. J. LUREK and D. B. CURLISS, in "Proceedings of the American Society for Composites, Twelfth Technical Conference," edited by R. F. Gibson and G. M. Newaz (Techonomic Publishing Co., Lancaster, PA, 1997) p. 1113.
8. R. J. MORGAN, R. J. JUREK, A. YEN and T. DONNELLAN, *Polymer* **34** (1993) 835.
9. M. A. CHAUDHARI, T. GALVIN and J. KING, *SAMPE J.* **21** (1985) 17.
10. B. J. LEE, M. A. CHAUDHARI and V. BLYAKHAM, *Polymer News* **13** (1988) 297.
11. R. J. MORGAN, in "Thermal Analyses of Polymers," edited by E. Turi (Academic Press, New York, NY, 1997) Ch. 9.
12. R. J. MORGAN, L. T. DRZAL, A. LEE and E. E. SHIN, Characterization of critical fundamental aging mechanisms of high temperature polymer matrix composites, AFOSR grant (1994–97).
13. R. J. MORGAN, in "Epoxy Resins and Composites, I," Advances in Polymer Science, edited by K. Dusek (Springer-Verlag, 1985), Vol. 12, Ch. 1.
14. J. E. LINCOLN, A. LEE, R. J. MORGAN and E. E. SHIN, *SAMPE Journal of Advanced Materials*, to be submitted.
15. CIBA-GEIGY, Plastics Department, Product Data Sheet, Matrimid 5292 System, 1985.
16. C. A. GAMLEN, E. D. CASE and D. K. REINHARD, *J. Appl. Phys. Letters* **59** (1991) 2529.
17. D. G. LEE, J. M. FITZ-GERALD and R. K. SINGH, *Surface Coatings & Tech.* **101** (1998) 187.
18. D. F. DIAO, K. KATO and K. HOKKIRIGAWA, *J. Triboloby-Trans. ASME* **116** (1994) 860.
19. C. LIU and E. D. CASE, *Experimental Mechanics* **37** (1997) 179.
20. C. LIU and E. D. CASE, *Experimental Techniques* **21** (1997) 28.
21. B. R. LAWN, in "Fracture Mechanics of Ceramics, Vol. 5," edited by R. C. Bradt, A. G. Evans, D. P. H. Hasselman and F. F. Lange (Plenum Press, New York, NY, 1983) p. 1.
22. J. LI, E. T. THOSTENSON, T. W. CHOU and L. RIESTER, *J. Eng. Mater. and Technology* **120** (1998) 152.
23. R. H. DOREMUS in "Glass Science" (John Wiley and Sons, New York, NY, 1973) p. 284.
24. I. M. LOW, G. PAGLIA and C. SHI, *J. Appl. Polymer Sci.* **70** (1998) 2349.
25. A. FLORES, F. J. BALTA CALLEJA and H. R. KRICHELDORF, *J. Mater. Sci.* **33** (1998) 3567.
26. G. M. PHARR, *Materials Science and Eng.* A **253** (1998) 151.
27. J. SUWANPRATEEB, *Polymer Testing* **17** (1998) 495.

Received 18 February
and accepted 24 August 1999